

Withaferin A and its Derivatives as Potential Anti-cancer Drug Lead Candidates: an In-silico Drug Design

Md. Reaz Uddin¹, Shibam Mondal², Shaikh Nazmul Haque², Subir Biswas³ and Jakir Ahmed Chowdhury¹

¹Department of Pharmaceutical Technology, Faculty of Pharmacy, University of Dhaka
Dhaka-1000, Bangladesh

²Pharmacy Discipline, School of Life Sciences, Khulna University, Khulna, 9208, Bangladesh

³Department of Pharmacy, Jagannath University, Dhaka-1100, Dhaka, Bangladesh

(Received: November 6, 2024; Accepted: May 21, 2025; Published (web): June 25, 2025)

ABSTRACT: The aim of the research is to identify novel bioactive molecules to treat breast and lung cancer, specifically natural Withaferin A and its structural analogues, utilizing the most advanced and reliable in-silico drug design methodologies. At the starting point of this work, the biological pass prediction score was computed to identify the target protein. The probability of the active (Pa) score is superior in antineoplastic agents (Pa: 0.916–0.942) compared to antifungal (Pa: 0.474–0.795) and antibacterial agents (Pa: 0.260–0.598). Consequently, oncogenic proteins associated with breast and lung cancer were identified, and the in-silico analysis proceeded. The docking scores of investigational medicines ranged from -7.3 to -7.8 kcal/mol for breast cancer-targeted protein PDB: 2W96 and from -7.4 to -8.4 kcal/mol for PDB: 4DNL. Conversely, the docking scores for regular palbociclib and tamoxifen were -7.8 kcal/mol and -8.4 kcal/mol, respectively. The docking scores of investigational drugs ranged from -7.6 to -9.2 kcal/mol for lung cancer-targeted protein PDB: 2IVS and from -8.5 to -9.8 kcal/mol for PDB: 3L9P. The docking scores for conventional Pralsetinib and Crizotinib were -9.4 kcal/mol and -8.9 kcal/mol, respectively. The docking score is critically significant, indicating that Withaferin A derivatives have superior docking scores to conventional chemotherapeutic drugs for breast and lung cancer. This experiment successfully assessed drug-likeness, ADME, and toxicity prediction, revealing that all compounds exhibited excellent human intestinal absorption, moderate solubility in aqueous medium, and were utterly free of hepatotoxicity and skin sensitization. Consequently, based on computational analysis, we believe that natural Withaferin A derivatives may serve as superior inhibitors in treating breast and lung cancer, warranting further experimental research.

Key words: Withaferin A; computer-aided drug design; breast cancer, lung cancer, molecular docking, ADMET.

INTRODUCTION

Cancer constitutes a significant global public health issue and ranks as the second leading cause of mortality following ischemic heart diseases worldwide.¹ The global burden of cancer is swiftly increasing as a result of continuous demographic and epidemiological transitions.² In 2022, around 20 million new cancer cases and 9.7 million cancer-related fatalities were reported.

Breast cancer and lung cancer were the most widespread cancers among women and men, respectively, in terms of both incidence and mortality.³ The prevalence of breast cancer and lung cancer is rising in affluent nations, and this burden is significantly transferring to at-risk populations in developing countries.⁴ While effective therapeutics for cancer remain elusive, various unconventional treatments such as radiotherapy, surgery, chemotherapy, alongside advanced technologies including gene therapy, stem cell therapy, natural antioxidants, targeted therapy and nanoparticles, are

Correspondence to: Jakir Ahmed Chowdhury
E-mail: jakir@du.ac.bd

Dhaka Univ. J. Pharm. Sci. 24(1): 105-120, 2025 (June)
DOI: <https://doi.org/10.3329/dujps.v24i1.82415>

currently employed for the diagnosis and treatment of cancer.⁵ The exploration of anticancer compounds from natural sources originates around 1550 BC. The scientific investigation of this subject is relatively recent, originating in the 1950s with the development of predominantly plant-derived anticancer drugs, such as alkaloid analogues.⁶ Natural products have traditionally played a crucial role in drug discovery due to their unique biocompatibility, novel structural frameworks, and diverse pharmacological characteristics.⁷⁻¹¹ Many anti-cancer pharmaceuticals are naturally occurring chemicals or synthetically produced derivatives of natural substances.¹² Nevertheless, chemotherapeutic agents often include detrimental side effects. Studies have demonstrated that natural and synthetic compounds exhibit various anticarcinogenic properties, such as inducing apoptosis in breast and lung cancer cells, inhibiting metastasis, and suppressing cellular proliferation.^{13,14}

Withaferin A (WA) is a significant withanolide that has established a prominent position in research due to its multifaceted biological features. It possesses anticancer, antioxidant, antifungal, antibacterial, hepatoprotective, hepatic disease therapy, and immunosuppressive properties.¹⁵ It is prevalent in the plant *Withania somnifera* Dunal, a significant medicinal plant used in Ayurvedic and indigenous medicine for millennia. Withaferin A is a 28-carbon withanolide with an ergostane framework and a δ -lactone structure.¹⁶ The qualitative structure-activity relationship (QSAR) indicates that it possesses two hydrogen bond donors and six hydrogen bond acceptors, which contribute to its high reactivity.

This computational study examines Withaferin A and its derivatives to evaluate their potential as treatments for breast and lung cancer. It aims to facilitate further development and the identification of new therapeutic agents. This strategy increases the chances of discovering effective therapies by identifying the most promising biomolecules early, hence mitigating expensive wet-laboratory failures.

COMPUTATIONAL METHOD AND WORKING PROCEDURE

Pass prediction. Pass prediction comprises the initial phase of evaluating the efficacy of a bioactive compound. The probabilities of being active (Pa) and inactive (Pi) are delineated. The likelihood of success rises as Pa increases and Pi falls; however, Pa and Pi will never be identical or equivalent. Pa and Pi grades can range from 0.00 to 1.00, with both Pa and Pi required to be less than 1. This method enables the differentiation of active compounds by screening pass prediction values, hence minimizing the time and expense associated with novel medication development. These novel chemical features should be expected in the early phases to ensure a comprehensive understanding of a particular molecule's efficacy.¹⁷⁻²⁰ Initially, pass prediction scores of five variants Withaferin A were gathered, along with its derivatives. Subsequently, we selected the four most potent compounds for further examination based on their maximal anticancer efficacy. The pass prediction data was obtained from the PASS website, <http://www.way2drug.com/passonline/>. Only the Pa values for Withaferin A and its derivatives have been compiled upon logging into the PASS online platform. (Table 1).

ADMET, drug-likeness and lipinski rule. The comprehensive pharmacokinetic parameters of Withaferin A and its derivatives were acquired from pkCSM (<https://biosig.lab.uq.edu.au/deeppk/data>) and SwissADME (<http://www.swissadme.ch/index.php>). The pkCSM was utilized to forecast pharmacokinetics, hence enhancing confidence in the reduced chance of novel drug compounds failing during clinical trials and increasing their likelihood of advancing as viable therapeutic candidates.²¹⁻²⁴ This section highlights human intestinal absorption, distribution, metabolism, excretion, water solubility, bioavailability, skin sensitivity, hepatotoxicity, carcinogenicity, and drug similarity. The Lipinski rule and drug similarity are crucial for formulating oral pharmaceuticals.²⁵ The optimized molecules were ultimately saved in pdb format for later computer research, including molecular docking.

This study indicates that Withaferin A and its analogues are potential therapeutic candidates for lung and breast cancer.

Ligand preparation and optimization. The preparation of ligands is a crucial element of molecular docking investigations. This necessitates the reorganization of atoms within the molecule until the configuration with the lowest ground-state energy is identified.²⁶ This step is crucial as molecular docking and molecular dynamics (MD) simulations require ligands with precise geometries²⁷. Initially, we obtained the chemical structures of Withaferin A and its analogues from the PubChem database in SDF format (Figure 1).²⁸ The configuration of each ligand was optimized at the B3LYP/6-31G level using density functional theory (DFT) in Gaussian 09.²⁹ Following optimization, we assessed the electronic properties, including the energy gap, hardness, softness, and the energies of the border orbitals—the

highest occupied molecular orbital (HOMO) and the lowest unoccupied molecular orbital (LUMO). These features demonstrate the chemical reactivity properties of the compounds.

Target protein preparation, ligands preparation and method of molecular docking. Molecular docking is a highly effective and pertinent method for assessing interactions of drug with proteins. Consequently, before the docking analysis, new protein must be prepared. The selection of proteins was based on commercially available lung and breast cancer drugs, targeting human proteins that interact with these drugs. Two proteins associated with breast cancer and two linked with lung cancer (PDB: 2W96, PDB: 4DNL, PDB: 2IVS, PDB: 3L9P) were selected. The three-dimensional proteins crystal structures were obtained from online sites (PDB or protein databank <https://www.rcsb.org/>) and are illustrated in Figure 2.³⁰

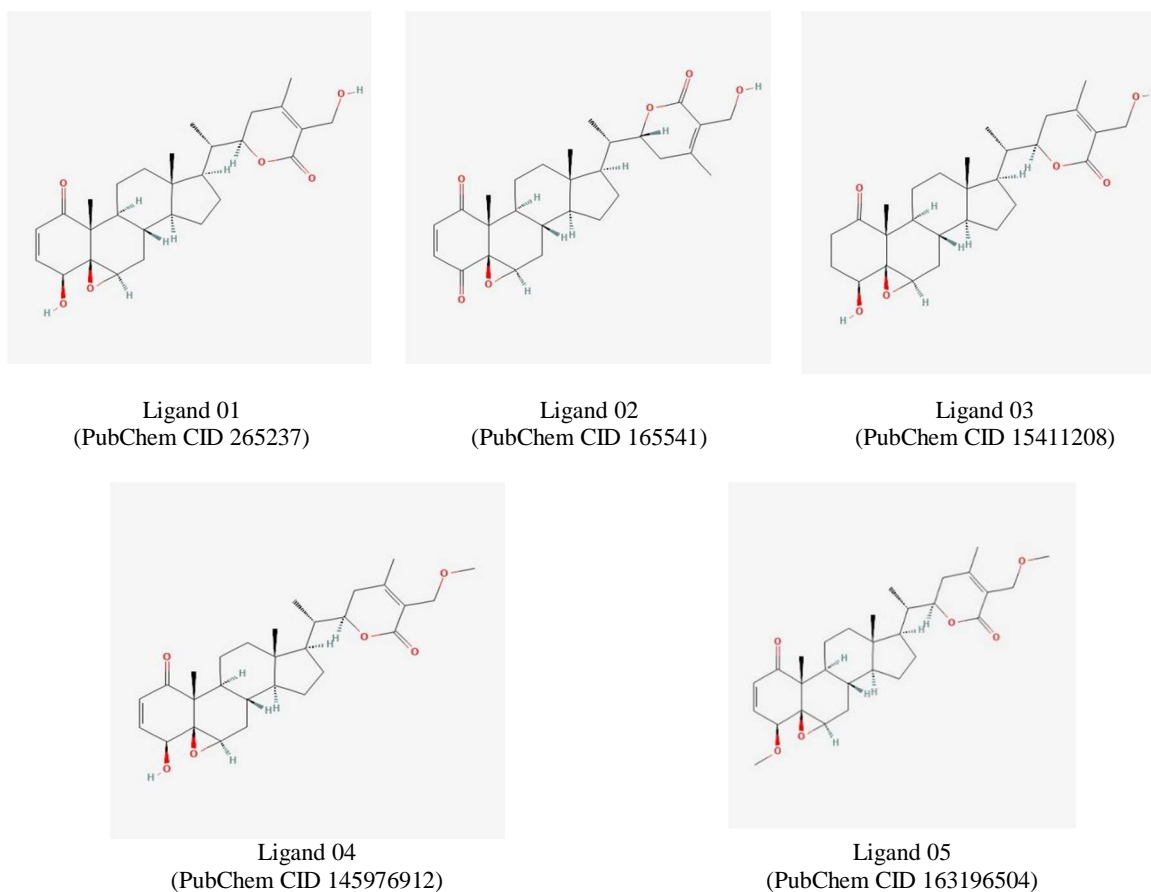


Figure 1. Chemical structure of Withaferin-A (Ligand 01) and its derivatives (Ligands 02 to 05)

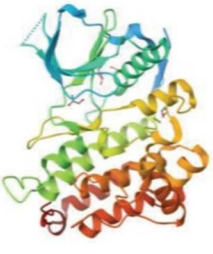
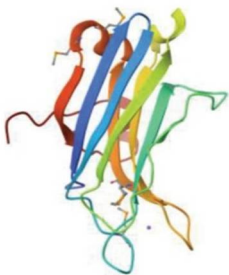
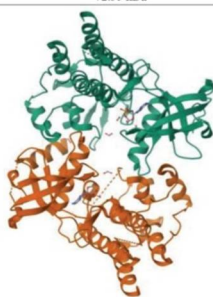
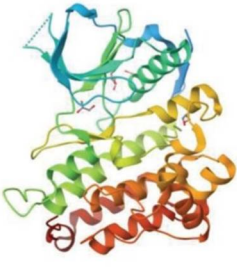
Title	Targeted protein for Breast Cancer PDB: 2W96	Targeted protein for Breast Cancer PDB: 4DNL
Organism	Homo sapiens	Homo sapiens
Method	X-Ray Diffraction	X-Ray Diffraction
Resolution	2.30 Å	1.90 Å
Total Structure Weight	65.67 kDa	16.48 kDa
3D dimensional structure of Breast Cancer Targeted Protein		
Title	Targeted protein for Lung Cancer PDB: 2IVS	Targeted protein for Lung Cancer PDB: 3L9P
Organism	Homo sapiens	Homo sapiens
Method	X-Ray Diffraction	X-Ray Diffraction
Resolution	2.00 Å	1.80 Å
Total Structure Weight	72.35 kDa	41.98 kDa
3D dimensional structure of Lung Cancer Targeted Protein		

Figure 2. Three-dimensional targeted protein structures

BIOVIA Discovery Studio 2021 was used to purify these proteins by eliminating all heteroatoms and water molecules, with the data then saved in PDB format. Energy minimization for these proteins was subsequently conducted using the Swiss PdbViewer 4.1.0 software, thereby preparing the proteins for molecular docking.³¹

For molecular docking, firstly, the purified and energy-optimized protein was uploaded into PyRx software and transformed into a macromolecule.³² Then, sequentially, the energy-minimized ligands (Ligand 01-05) and conventional drugs (Palbociclib, Tamoxifen, Pralsetinib, Crizotinib) were uploaded in PDB format through Gabedit software. Finally, the binding affinity (kcal/mol) with Withaferin A, its derivatives, and conventional drugs with respect to the diseases was recorded and analyzed.

RESULTS AND DISCUSSION

Structure-activity relationship and optimized structure of ligand. It is possible to predict the necessary biological activity derived from the molecular structure utilizing the structure-activity relationship (SAR). There is a correlation between pharmaceuticals and chemical design. This advanced technology is applied in drug development to facilitate the discovery or manufacture of novel molecules and to enhance the characterization of existing medicinal substances. In the studies we conducted, Withaferin A served as the principal molecule. We substituted various powerful functional groups at different positions of Withaferin-A to evaluate its efficacy in response to breast and lung carcinoma. The molecular configuration is illustrated in figure 2.

Geometry optimization is accomplished by altering the atomic arrangement of a molecule to acquire the best stable conformation with the lowest possible ground-state energy.³³ This approach is predominantly utilized in computational chemistry.

Before performing molecular docking, it is essential to optimize all tested ligands to obtain accurate results. Figure 3 illustrates and displays the optimized chemical structures.

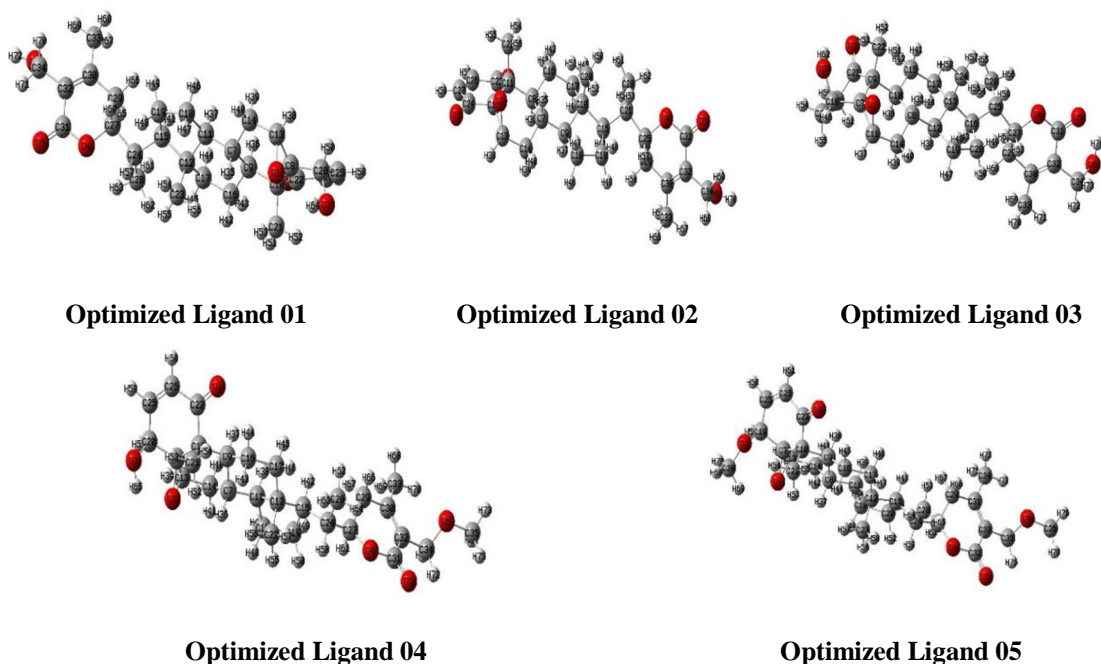


Figure 3. Optimized structure of Withaferin-A (Ligand 01) and its structural analogues (Ligands 02 to 05).

Pass prediction. The online tool PASS (Prediction of Activity Spectra for Compounds; <http://www.pharmaexpert.ru/PASSonline/>) was utilized to obtain data regarding the cytostatic, breast cancer, colon cancer, lung cancer, colorectal cancer and antineoplastic efficacy of the compounds derived from SAR research. The collecting of pass spectrum data, with Pa scores ranging from 0.916 to 0.942 for antineoplastic, 0.256 to 0.948 for cytostatic, 0.645 to 0.722 for breast cancer, 0.520 to 0.672 for lung cancer, 0.595 to 0.672 for colorectal cancer and 0.478 to 0.594 for colon cancer were analyzed. The likelihood of exhibiting pharmacological activity or a higher Pa score for anticarcinogenic agents is presented here. Therefore, the diseases of lung cancer as well as breast cancers have been chosen as targeted diseases, and additional related investigations were conducted (Table 1).

Lipinski rule, pharmacokinetics and drug likeness. Drug-likeness is a qualitative characteristic utilized in drug design to evaluate the degree to which a substance demonstrates "drug-like" properties, particularly concerning variables such as bioavailability. Pharmacokinetics is the examination of how an organism influences a medicine. In 1997, Christopher A. Lipinski established the drug-likeness prediction model, which assesses whether a chemical molecule demonstrating particular pharmacological or biological activity has the chemical and physical qualities conducive to human oral bioavailability. Drug-likeness methodologies and Lipinski's Rule of Five (which specifies that a molecule must possess a molecular weight below 500 Daltons, no more than 10 hydrogen bond acceptors, a maximum number of 5 hydrogen bond donors, and an octanol-water partition coefficient log P not surpassing 5) facilitate

the prediction of pharmacokinetic parameters derived from the compound's structure. These attributes are essential in drug discovery and assist in defining the drug-like properties of the ligands.²⁵ Ligand structure files were uploaded to the SwissADME website to get the properties and evaluations of the Lipinski rules. The identified chemicals meet this requirement.³⁴

The molecular weights of Withaferin A (L01) and its derivatives (L02-L05) ranged from 468.60 to

498.60. The hydrogen bond donor was 0-2, the hydrogen bond acceptor was 06, and the octanol–water partition coefficient log P was 3.42-4.28. Therefore, Withaferin A and all of the selected derivatives in the current study adhere to Lipinski's rule of five. As illustrated in table 3, the pharmacological characteristics of all the ligands exhibit positive effects.

Table 1. Biological pass prediction score of Withaferin-A and its derivatives

Ligand no.	PubChem CID	Antineoplastic	Cytostatic	Lung cancer	Breast cancer	Colon cancer	Colorectal cancer
		Pa	Pa	Pa	Pa	Pa	Pa
L01	265237	0.916	0.256	0.552	0.722	0.508	0.511
L02	165541	0.942	0.905	0.588	0.704	0.594	0.595
L03	15411208	0.929	0.920	0.587	0.665	0.481	0.485
L04	145976912	0.919	0.948	0.520	0.686	0.478	0.481
L05	163196504	0.937	0.916	0.672	0.645	0.521	0.522

Table 2. Lipinski rule data, pharmacokinetics and evaluation of drug likeness

Ligand No.	Molecular weight (g/ mol)	Rotatable bonds	Hydrogen bond donor	Hydrogen bond acceptor	Molar refractivity	Consensus log po/w	Drug likeness (lipinski rule)	
							Result	Violation
L01	470.60	3	2	6	127.49	3.42	Yes	0
L02	468.60	3	1	6	126.53	3.65	Yes	0
L03	472.60	3	2	6	127.96	3.60	Yes	0
L04	484.62	4	1	6	132.22	3.85	Yes	0
L05	498.60	5	0	6	136.95	4.28	Yes	0

Thermodynamic analysis. Thermochemical calculations help predict reaction kinetics and chemical stability. Primarily, free energy and enthalpy pertain to the absorption or release of energy during a chemical process and the chemical stability of a molecule.³⁵ The free energy value is crucial in investigating binding potential with other compounds, as both the sign and magnitude exhibit distinctive properties of a compound. The negative sign indicates spontaneous binding, while the high value suggests greater availability of bonds. All molecules' free energy and enthalpy values are

negative (Table 3). External energy is not required for bindings.

The highly electronegative molecule (oxygen) is present in all analogues of *Withaferin A* and *Withaferin A*. The thermodynamic properties of Withaferin A and its analogues are characterized by elevated energy values (internal and free energy) and negative enthalpy values. The enthalpy values ranged from -1538.854 Hartree to -1618.561 Hartree. The dipole moment is crucial for characterizing a molecule's electronic properties. A high dipole moment value of a molecule enhances intermolecular interactions. A high dipole moment indicates a more

excellent polar character.^{36,37} Withaferin A and its derivatives exhibit a significantly high dipole moment, indicating a significant binding affinity of

the molecule, the formation of hydrogen bonds and non-covalent interactions in the drug-receptor complex.³⁸ (Table 3).

Table 3. Molecular formula, molecular weight, energies and dipole moment of Withaferin A and its analogues.

Ligand no.	PubChem CID	Molecular Formula	Molecular weight	Internal energy (Hartree)	Enthalpy (Hartree)	Free energy (Hartree)	Dipole moment (Debye)
L01	265237	C ₂₈ H ₃₈ O ₆	470.60	-1540.035	-1540.034	-1540.129	7.172
L02	165541	C ₂₈ H ₃₆ O ₆	468.60	-1538.85	-1538.854	-1538.949	4.991
L03	15411208	C ₂₈ H ₄₀ O ₆	472.60	-1541.234	-1541.233	-1541.329	8.249
L04	145976912	C ₂₉ H ₄₀ O ₆	484.62	-1579.301	-1579.300	-1579.399	7.317
L05	163196504	C ₃₀ H ₄₂ O ₆	498.60	-1618.562	-1618.561	-1618.664	8.246

Frontier molecular orbitals and quantum calculation (HOMO-LUMO). All five ligands were examined to reveal the computed values of HOMO and LUMO: energy gap, hardness and softness for all compounds (Table 4). The values were calculated via the DFT/B3LYP method with a 6-31G basis set. The energies calculated from HOMO-LUMO are critical determinants of molecular chemical reactivity, as elucidated by frontier molecular orbital theory principles. The gap from HOMO-LUMO is correlated with each molecule's chemical hardness, softness, chemical potential and electrophilic index. A more significant energy gap between the HOMO and LUMO enhances kinetic stability and diminishes chemical reactivity in a molecule. On the contrary, a narrow HOMO-LUMO gap indicates reduced chemical stability. It facilitates the efficient flow of electrons between a high LUMO and a depressed HOMO in chemical processes.^{39,40} The analysis demonstrated that the compound CID: 165541 showed the most negligible energy gap (ΔE) relative to the remaining compounds. The findings indicate a higher level of chemical reactivity and significant

intramolecular charge transfer between an electron-donating group and an electron-accepting group. The gaps found from HOMO-LUMO calculation range from 3.946 eV to 5.361 eV (Table 4). Furthermore, table 5 presents numeric values for the softness criterion. The elements exhibiting greater softness values are characterized by more fast degradation. Thus, they take considerably a lesser amount of time to modify their arrangement of electron configuration. Contrarywise, hardness is a critical characteristic of a molecule. Typically, substances with elevated hardness ratings demonstrate increased resistance to alterations in their electron configuration. The values of hardness and softness are inversely correlated. The hardness values are considerably higher than the softness values for all compounds except the CID: 165541 compounds. Compounds CID: 165541 exhibit comparatively elevated softness values. This indicates that their decomposition may transpire swiftly compared to other chemicals. Figure 4 illustrates the HOMO-LUMO diagram.

Table 4. Energy (eV) of HOMO-LUMO, gap, hardness (η), softness (S), chemical potential (μ), electronegativity (χ), and electrophilicity (ω) of Withaferin A and its analogues.

Ligand No.	PubChem CID	eHOMO (eV)	eLUMO (eV)	Gap	hardness (η)	softness (S)	chemical potential (μ)	electronegativity (χ)	electrophilicity (ω)
L01	265237	-6.857	-2.014	4.844	2.422	0.413	-4.435	4.435	4.062
L02	165541	-7.048	-3.102	3.946	1.973	0.507	-5.075	5.075	6.527
L03	15411208	-6.912	-1.551	5.361	2.680	0.373	-4.231	4.231	3.340
L04	145976912	-6.803	-2.014	4.789	2.395	0.418	-4.408	4.408	4.058
L05	163196504	-6.694	-1.959	4.735	2.367	0.422	-4.327	4.327	3.954

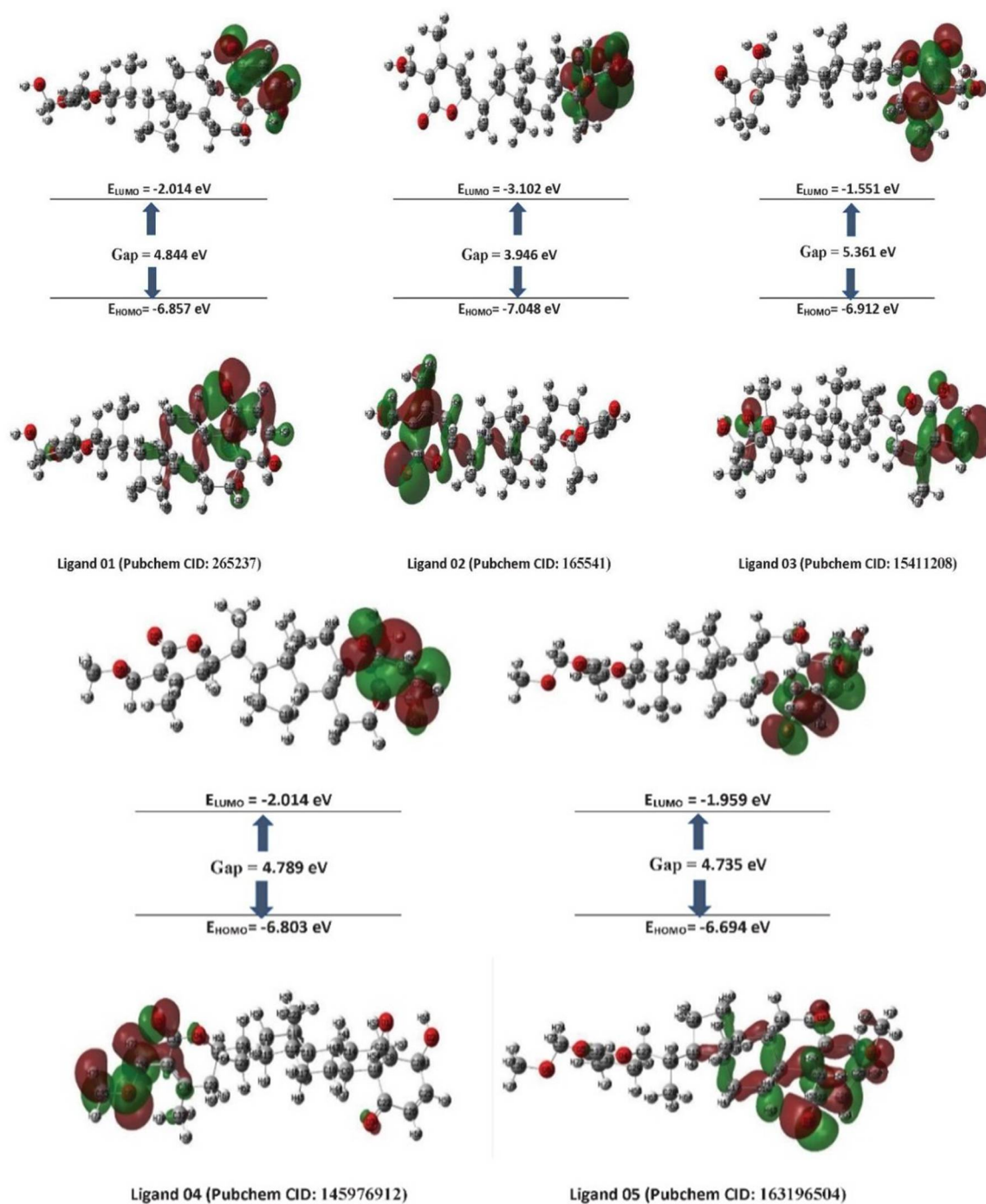


Figure 4. HOMO-LUMO and energy gap diagram

Molecular electrostatic potential (MEP) charge distribution map. The molecular electrostatic potential (MEP) map illustrates the cumulative charge of electrons and nuclei, providing insight into the characteristics of electronegativity, partial charge dipole moment and molecular

reactivity.^{41,42} It offers perspectives into the electrophilic and nucleophilic domains of molecules by examining the potential energy distribution generated by the electrons and nuclei of the molecule. MEP functions as a static distribution of potential and assists in delineating and forecasting the functional

behavior of a chemical. Electrostatic potentials have been essential in exploring various phenomena in biological, physical, and associated disciplines. Figure 5 depicts the dynamically computed MEP values for compounds (1-5) of Withaferin A and its derivatives, anticipated via the DFT approach. In this depiction, the red hue signifies the lowest intensity of electrostatic potential energy, denoting the most pronounced negative region and the site most

vulnerable to electrophilic assaults. Contrarywise, the blue zone in the MEP denotes the peak value of the potential electrical charge, suggesting both the maximal positive region and a site conducive to nucleophilic substitution, as illustrated in figure 5. The MEP map indicates that the oxygen atom exhibits the biggest negative potential, whereas the hydrogen atom displays the highest positive potential.

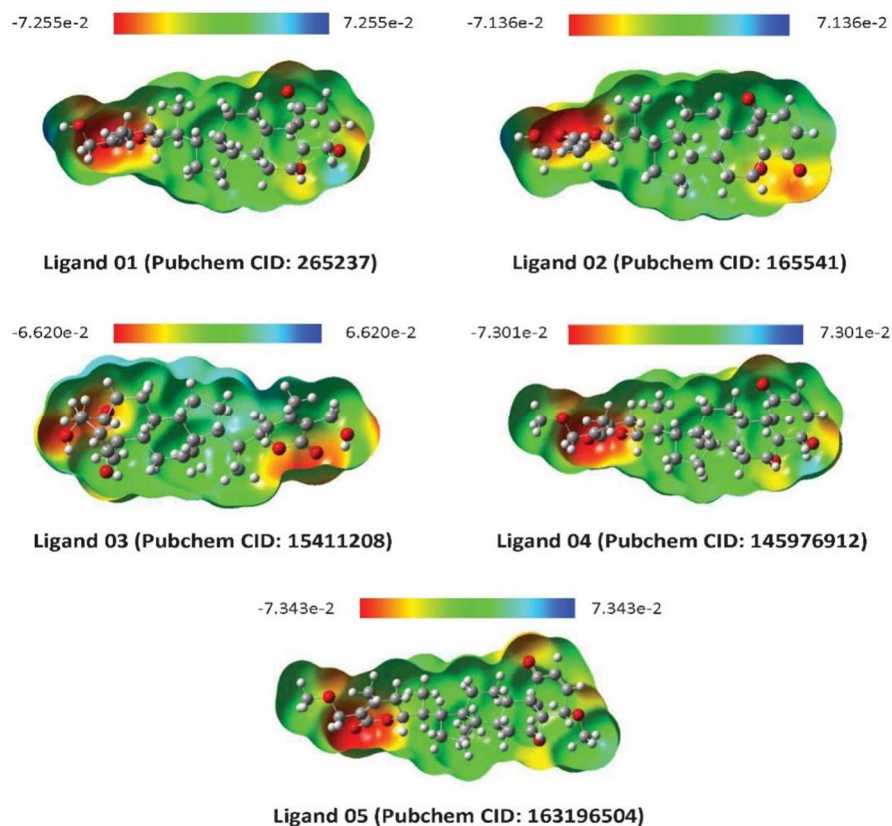


Figure 5. Molecular electrostatic potential map of Withaferin A analogues Molecular docking against targeted protein

Molecular docking and interaction analysis.

Docking is considered one of the most promising methodologies in computer-aided drug design.⁴³ This method forecasts the optimal orientation of a chemical when it binds to a protein with ligands to establish a stable complex.⁴⁴ Docking may potentially reveal the binding of a small molecule ligand to the relevant target region during the formation of complex of drug and protein.⁴⁵ The drug is considered as a standard medicine when the molecular docking score is above -6.000 kcal/mol.²²

Molecular docking tests were utilized to validate the pharmacological properties and potential binding affinities of compounds 1-5 for proteins associated with breast and lung cancer. The conventional medications palbociclib and tamoxifen for breast cancer and pralsetinib and crizotinib for lung cancer were examined for binding affinity using docking studies and compared with Withaferin A and its derivatives. Our analysis revealed significant affinities of the experimental candidates for the targeted protein compared to conventional medicines.

The designated proteins for breast cancer were PDB: 2W96 and PDB: 4DNL, whereas those for lung cancer were PDB: 2IVS and PDB: 3L9P. Protein selection was predicated on the standard medication and its functional protein.

The binding affinities of Withaferin A and its derivative with the breast cancer-targeted protein PDB: 2W96 ranged from -7.3 to -7.8 kcal/mol, with a maximum binding score of -7.8 kcal/mol achieved for ligand 01. The binding affinity of the standard drug Palbociclib with the same protein PDB: 2W96 was -7.7 kcal/mol. A different protein associated with breast cancer was examined, revealing that the binding affinities of potential compounds ranged from -7.4 to -8.4 kcal/mol, significantly surpassing the binding affinity of that protein with the conventional medication tamoxifen, which was -5.9

kcal/mol. The optimal binding affinity was -8.4 kcal/mol, exhibited by ligand 02.

The binding affinity range of prospective therapeutic compounds with the lung cancer-targeted proteins PDB: 2IVS and PDB: 3L9P was -7.6 to -9.2 kcal/mol and -8.5 to -9.8 kcal/mol, respectively. The binding affinities for the conventional medicines Pralsetinib and Crizotinib were -9.4 kcal/mol and -8.9 kcal/mol, respectively. In both cases, ligand 02 exhibited significant binding affinity with the proteins targeted for cancer, with the highest affinity observed for 3L9P. This indicated that these bioactive compounds may be effective anticancer agents for lung and breast cancer. In all four proteins of breast and lung cancer, the newly created biomolecules exhibit superior and promising efficacy (Table 5).

Table 5. Binding affinity of candidate and standard drug against the targeted protein for breast and lung cancer

Ligand No./drug	PubChem CID	Binding affinity (kcal/mol)			
		Targeted protein for breast cancer		Targeted protein for lung cancer	
		PDB: 2W96	PDB: 4DNL	PDB: 2IVS	PDB: 3L9P
Candidate Drug					
L01	265237	-7.8	-7.6	-8.4	-9.0
L02	165541	-7.7	-8.4	-9.2	-9.8
L03	15411208	-7.7	-7.4	-8.1	-8.5
L04	145976912	-7.3	-7.5	-8.5	-9.4
L05	163196504	-7.5	-7.5	-7.6	-8.5
Existing standard drug					
Palbociclib	5330286	-7.7	---	---	---
Tamoxifen	2733526	---	-5.9	---	---
Pralsetinib	129073603	---	---	-9.4	---
Crizotinib	11626560	---	---	---	-8.9

Interactions of ligands-proteins and analysis of the active site. The BIOVIA Discovery Studio Visualizer was employed to examine the molecular interactions between the chemicals and the macromolecules. For clarity, each protein-specific standard drug complex and candidate ligand-protein was chosen according to the highest binding affinity to the corresponding protein receptors. Subsequently, we conducted a comprehensive screening of the five

experimental ligand-protein complexes alongside the four-standard drug-protein complexes to identify and assess their active amino acid residues and binding sites.

In the breast target protein (PDB: 2W96)-ligand 01 binding complex, the active amino acids identified were GLU A: 70 and LYS A: 72. Conversely, the conventional drug Palbociclib formed four connections with the protein at THR A: 184, GLU A:

75, SER A: 258, and PHE A: 78 (Figure 6). Another target protein (PDB: 4DNL) for breast cancer has been complexed with Ligand 02, with three active binding sites: ASP A: 254, PRO A: 188, ARG A: 216. The binding affinity of the standard medicine tamoxifen is -5.9 kcal/mol, which is much lower compared to the investigational molecule ligand 02, with a binding affinity of -8.4 kcal/mol, as illustrated

in the 2D representation of the complex. In the protein-drug complex, four bonds were established: LYS A: 230, LEU A: 200, one alkyl bond at LYS A: 232, and one pi-carbon bond at LYS A: 232. The bond lengths were longer in the investigational drug complex, and the absence of strong hydrogen bonds supported the lower binding affinity of standard drug (Figure 7).

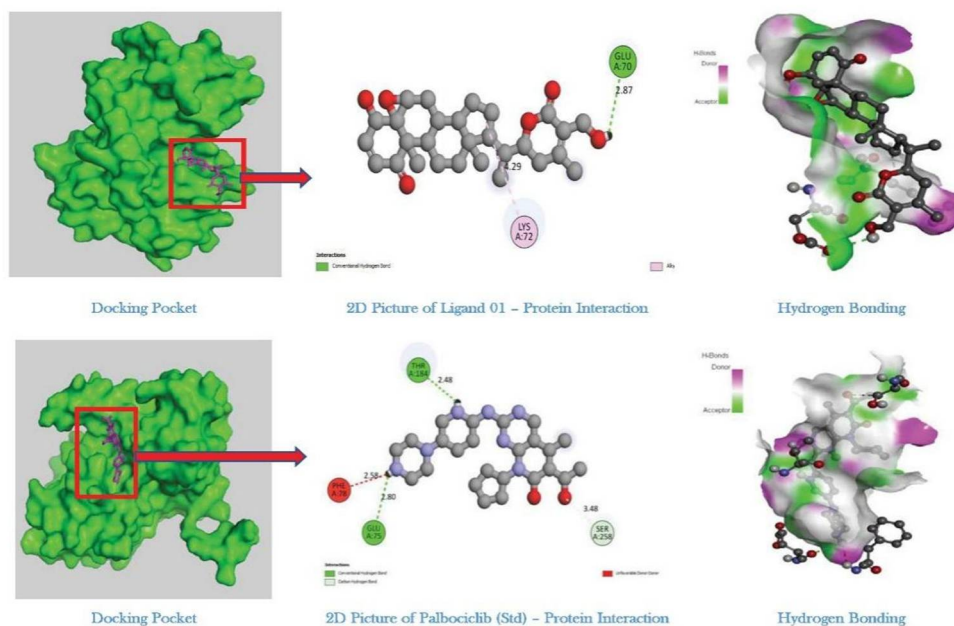


Figure 6. Comparative molecular docking poses of breast cancer targeted protein (4DNL) with ligand 01 (265237) and standard drug Palbociclib

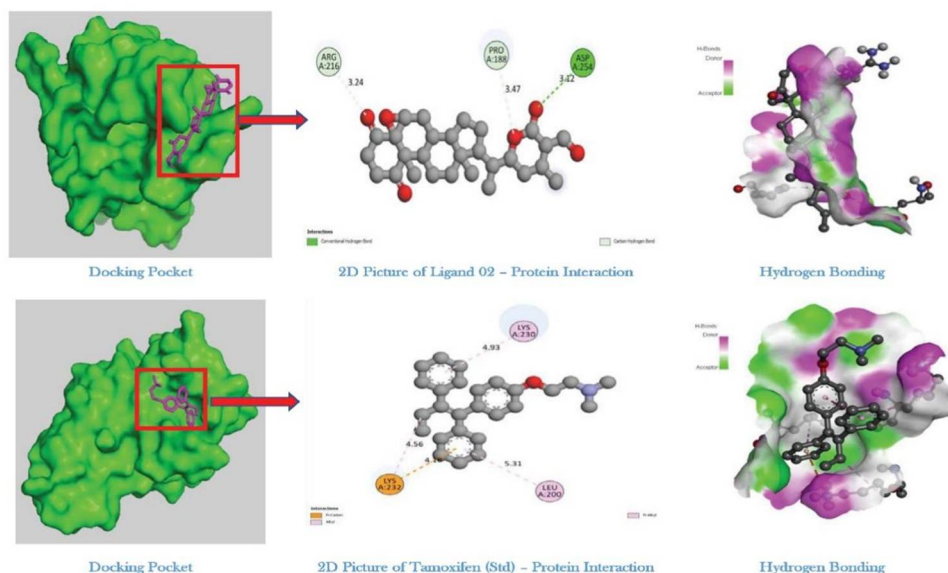


Figure 7. Comparative molecular docking poses of breast cancer targeted protein (4DNL) with ligand 02 (165541) and standard drug tamoxifen

In the instance of the ligand 02-lung cancer targeted protein (2IVS), a binding site comprising nine (9) amino acids is produced with varying binding lengths. Conversely, the current medicine Pralsetinib binds to the proteins via only three amino acids: ASP A: 771, ASP A: 898, and ASN A: 777 (Figure 8). The standard treatment, Crizotinib, and its

lung cancer-targeted protein (3L9P) were examined, revealing that in complex with ligand 02, ten distinct types of bonds with amino acids were formed. In contrast, in complex with the standard, only one specific amino acid binding site was produced (Figure 9).

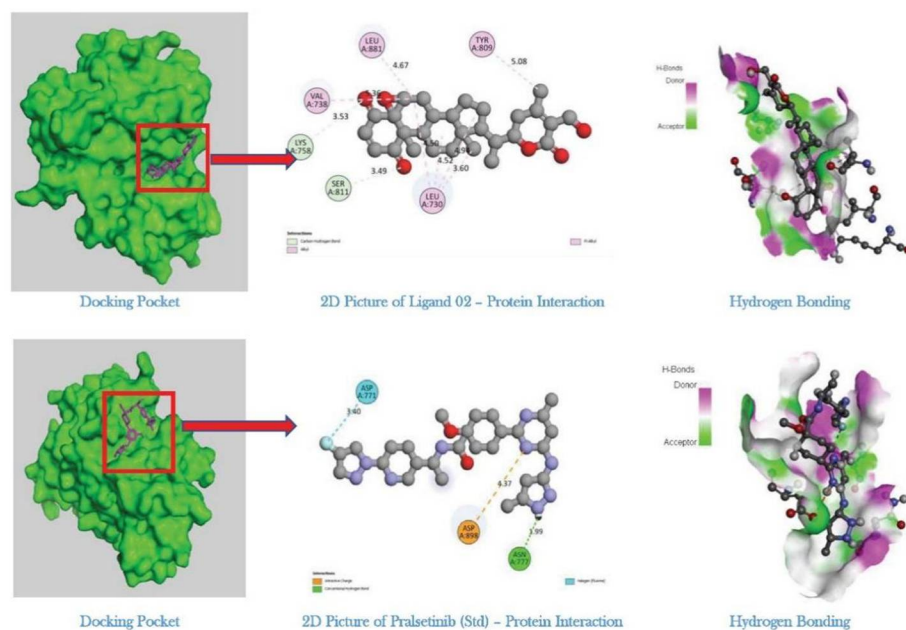


Figure 8. Comparative molecular docking poses of lung cancer targeted protein (2IVS) with Ligand 02 (165541) and standard drug Pralsetinib.

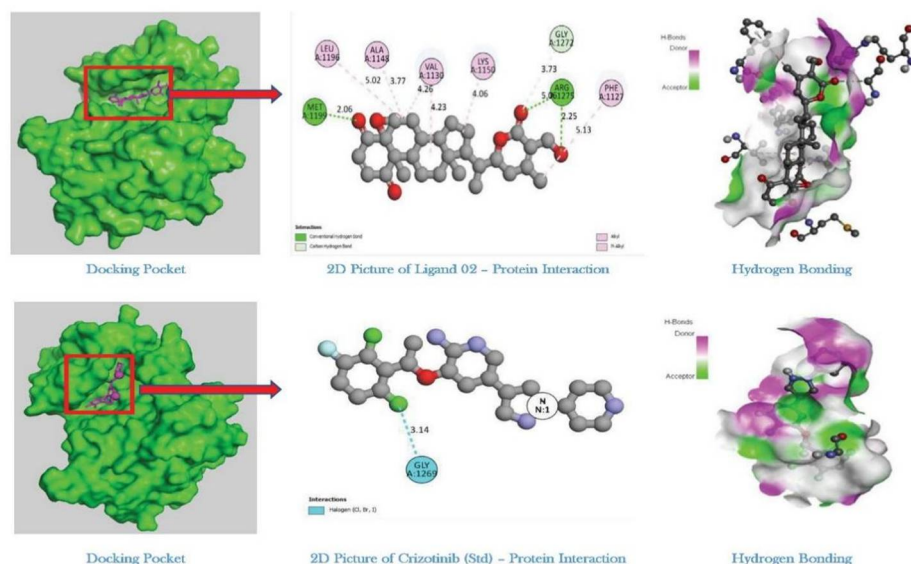


Figure 9. Comparative molecular docking poses of lung cancer targeted protein (3L9P) with Ligand 02 (165541) and standard drug Crizotinib.

Computational ADME data prediction.

Computational ADMET (Absorption, distribution, metabolism, excretion, and toxicity) data prediction plays an essential role in pharmaceutical development. A significant proportion of medicines fail clinical trials due to inadequate ADMET characteristics. The pkCSM web server was utilized to forecast the ADMET profiles of our chosen chemicals (Table 2).

We emphasized the primary absorption characteristics: 'water solubility' and 'absorption in the human gut.' Solubility is quantified using the Log S scale: insoluble: <-10 ; poor: <-6 ; moderate: <-4 ; soluble: <-2 ; and very high: <0 .^{24,46,47} Most compounds demonstrated moderate water solubility with Log S values below -6 . The results indicated that the aqueous solubility varies from -5.063 to -5.716 , suggesting they are moderately soluble. Furthermore, all potential drug candidates exhibit an excellent absorption rate within the human gastrointestinal tract. A range of values represents it

from 85.345% to 100.000%. In addition, all molecules showed outstanding absorption rates, with compound CID: 145976912 and compound CID: 163196504 being the most promising at 98.002% 100%, respectively.

The drug's distribution within the body is crucial to measuring its transfer from the bloodstream to the tissues.⁴⁸ The volume of distribution (VDss) values less than -0.15 signify inadequate distribution. Values beyond 0.45 signify a greater distribution.⁴⁸ In our investigation, certain chemicals exhibited intermediate VDss values, whilst others displayed low VDss values ranging from -0.131 to -0.035 .

We examined the metabolic characteristics of the substances. In this context, the isoforms of cytochrome P450, specifically CYP450 1A2 and CYP2C9 substrates, are considered. These enzymes are crucial for the metabolism of drugs.^{49,50} Since almost all candidates show excellent absorption, no drugs were predictively capable of inhibiting CYP450 1A2 and CYP2C9.

Table 6. Summary of ADME data for selected Withaferin A derivatives

Ligand no.	Absorption		Distribution	Metabolism	Excretion	Toxicity						
	Water solubility Log S	Caco-2 permeability (10 ⁻⁶ cm/s)	Human Intestinal Absorption (%)	BBB Permeability (log BB)	CYP450 1A2 Inhibitor	CYP450 2C9 Inhibitor	Total Clearance (ml/min/kg)	Renal OCT2 substrate	Max. tolerated dose (log mg/kg/day)	Skin Sensitization	Hepatotoxicity	
L01	-5.063	0.829	85.345	-0.131	-0.03	No	No	0.435	Yes	-0.695	No	No
L02	-5.21	0.873	90.629	-0.103	-0.353	No	No	0.338	Yes	-0.568	No	No
L03	-5.132	0.82	86.198	-0.126	-0.031	No	No	0.449	Yes	-0.696	No	No
L04	-5.42	0.862	98.022	-0.031	-0.427	No	No	0.434	No	-0.515	No	No
L05	-5.716	0.856	100.00 0	-0.035	-0.499 -0.499	No	No	0.458	No	-0.367	No	No

Total clearance and renal OCT2 substrate are critical parameters for a drug's excretion profile.⁵¹ It serves to forecast the maximum dosage of drug a patient may administer during a specified timeframe.^{52,53} The total clearance rates are found from 0.338 to 0.458 log mg/kg/day, of which the

maximum value of 0.458 log mg/kg/day of the drug can be cleared from the body, and the minimum value is 0.338 log mg/kg/day. Finally, ligand 01-03 can be eliminated via the renal OCT2 substrate, whereas ligand 04 and ligand 05 cannot be excreted. (Table 2).

Finally, the maximum tolerated dose (MTD) was analyzed. It is used to forecast the maximum amount of medicine a patient can take in a given period.^{52,53} In this study, all the compounds showed negative values (in terms of log mg/kg/day) that were clearly less than 0.477, indicating minimal toxicity.

CONCLUSIONS

This research has enhanced and strengthened Withaferin A and its derivatives as novel pharmacological agents for anti-breast cancer and anti-lung cancer applications by computer-aided procedures, employing various computational techniques against the specific target proteins associated with the diseases.

A thorough analysis demonstrates that Withaferin A and its four derivative compounds exhibit substantial inhibitory effects due to their binding affinities. Ligand 01 exhibited the highest binding affinity score for the breast cancer-targeted protein PDB: 2W96, measured at -7.8 kcal/mol, surpassing the affinity of the standard medication. Conversely, ligand 02 exhibited a binding affinity of -8.4 kcal/mol for the breast cancer-targeted protein PDB: 4DNL, which was much superior to the traditional medication tamoxifen. In contrast to lung cancer, ligand 02 had the highest affinity scores of -9.2 and -9.8 kcal/mol for the targeted proteins PDB: 2IVS and PDB: 3L9P, respectively.

Furthermore, the drug-likeness of all substances is broadly acknowledged. Therefore, the pharmaceutical research and application process may be directed by forecasting the in-silico modeling of ADMET characteristics for safe drugs. Additionally, it achieved an enhanced ADMET profile for all compounds, exhibiting low toxicity and moderate solubility; nearly all candidate medications demonstrate exceptional intestinal absorption and the ability to pass through the blood-brain barrier, with minimal metabolism by CYP450 1A2 and CYP450 2C9 inhibitors. The lower renal clearance of the proposed medications indicates prolonged anti-cancer action without requiring frequent administration. Furthermore, the absence of adverse reactions related

to skin sensitization and hepatotoxicity supports the safety of patient use.

This study suggests that Withaferin A and its derivatives demonstrate promising computational efficacy as breast and lung cancer treatments. This computational study provides valuable results regarding the proteins associated with breast and lung cancer. It is recommended that additional experimental investigations be performed to assess the actual effectiveness on a larger scale.

AUTHOR CONTRIBUTIONS

Md Reaz Uddin: Conceptualization (lead); data curation (equal); investigation (equal); methodology (lead); visualization (equal); writing – original draft (lead). **Shibam Mondal:** Conceptualization (equal); data curation (equal); formal analysis (equal); validation (equal); visualization (equal); writing – original draft (equal). **Shaikh Nazmul Haque:** Formal analysis (equal); investigation (equal); software (equal). **Subir Biswas:** Data curation (equal); formal analysis (equal); investigation (equal); software (equal). **Dr. Jakir Ahmed Chowdhury:** Project administration (lead), supervision (lead); validation (equal); writing – review and editing (lead).

Data availability statement

The original contributions highlighted in the study are incorporated in the article/Supplementary material. Additional inquiries may be sent to the corresponding authors.

Conflict of interest

The authors declare that the research was performed without any commercial or financial affiliations that might be interpreted as a potential conflict of interest.

Funding

This project did not receive any funds.

REFERENCE

- Harding, M. C. et al. 2018. Transitions from heart disease to cancer as the leading cause of death in US states, 1999-2016. *Prev. Chronic. Dis.* **15**, E158.
- Mattuzzi, C. and Lippi, G. 2019. Current cancer epidemiology. *J. Epidemiol. Glob. Health* **9**, 217-222.
- Bray, F., Laversanne, M., Sung, H., Ferlay, J., Siegel, R. L., Soerjomataram, I. and Jemal, A. 2024. Global cancer statistics 2022: GLOBOCAN estimates of incidence and mortality worldwide for 36 cancers in 185 countries CA: A *Cancer J. Clin.* **74**, 229-263.
- Francies, F. Z., Hull, R., Khanyile, R. and Dlamini, Z. 2020. Breast cancer in low-middle income countries: abnormality in splicing and lack of targeted treatment options. *Am. J. Cancer Res.* **10**, 1568-1591.
- Kaur, R., Bhardwaj, A. and Gupta, S. 2023. Cancer treatment therapies: traditional to modern approaches to combat cancers. *Mol. Biol. Rep.* **50**, 9663-9676.
- Asma, S. T. et al. 2022. Natural products/bioactive compounds as a source of anticancer drugs. *Cancers* **14**, p.6203.
- Ahmed, N. U. 2023. Exploration of controlled hypoglycemic effect in streptozotocin-induced type 1 diabetes and antibacterial activity of combination of ethanolic extract of garlic (*allium sativum*) and ginger (*zingiber officinale*) stem; *In vivo* studies supported by in silico study. *Biomed. J. Sci. Tech. Res.* **51**, 42628-42637.
- Mondal, S., Hossain, I. and Islam, M. N. 2017. Determination of antioxidant potential of *cucurbita pepo* Linn. (An edible herbs of Bangladesh). *J. Pharmacogn. Phytochem.* **6**, 1016-1019.
- Shawon, N. J. et al. 2024. *In vivo* and *in silico* analysis of antihypertensive activities of *Ficus religiosa* fruit extract. *Dhaka Univ. J. Pharm. Sci.* **23**, 23-36.
- Tahsin, M. R. et al. 2021. An evaluation of pharmacological healing potentialities of Terminalia Arjuna against several ailments on experimental rat models with an in-silico approach. *Heliyon* **7**, 1-17.
- Tahsin, Md. R. et al. 2022. *In Vivo* and in silico assessment of diabetes ameliorating potentiality and safety profile of Gynura procumbens Leaves. *Evid. Based. Complement Alternat. Med.* **2022**, 1-18.
- Chaachouay, N. and Zidane, L. 2024. Plant-derived natural products: a source for drug discovery and development. *Drugs and Drug Candidates* **3**, 184-207.
- Anand, U. et al. 2022. Cancer chemotherapy and beyond: Current status, drug candidates, associated risks and progress in targeted therapeutics. *Genes. Dis.* **10**, 1367-1401.
- Paul, S. et al. 2021. Withania somnifera (L.) Dunal (Ashwagandha): A comprehensive review on ethnopharmacology, pharmacotherapeutics, biomedicinal and toxicological aspects. *Biomedicine & pharmacotherapy = Biomedecine & pharmacotherapie* **143**, 112175.
- Sultana, T. et al. 2021. Withaferin A: From Ancient Remedy to Potential Drug Candidate. *Mol.* **26**, 7696.
- Fang, S.T., Liu, J.K. and Li, B. 2012. Ten new withanolides from physalis peruviana. *Steroids* **77**, 36-44.
- Filimonov, D. A. et al. 2014. Prediction of the biological activity spectra of organic compounds using the pass online web resource. *Chem. Heterocycl. Comp.* **50**, 444-457.
- Lagunin, A., Stepanchikova, A., Filimonov, D. and Poroikov, V. 2000. PASS: prediction of activity spectra for biologically active substances. *Bioinform.* **16**, 747-748.
- Poroikov, V. V. et al. 2003. PASS biological activity spectrum predictions in the enhanced open NCI database browser. *J. Chem. Inf. Comput. Sci.* **43**, 228-236.
- Ivanov, S. M., Lagunin, A. A., Rudik, A. V., Filimonov, D. A. and Poroikov, V. V. 2018. ADVERPred-web service for prediction of adverse effects of drugs. *J. Chem. Inf. Model.* **58**, 8-11.
- Daina, A., Michielin, O. and Zoete, V. SwissADME: a free web tool to evaluate pharmacokinetics, drug-likeness and medicinal chemistry friendliness of small molecules. *Sci. Rep.* **7**, 42717.
- Islam, Md. R. et al. 2024. Ligand-based drug design against Herpes Simplex Virus-1 capsid protein by modification of limonene through in silico approaches. *Sci. Rep.* **14**, 9828.
- Uzzaman, M. et al. 2021. Physicochemical, spectral, molecular docking and ADMET studies of Bisphenol analogues; A computational approach. *Inform. Med. Unlocked.* **25**, 100706.
- Tayyeb, J. Z. et al. 2024. Identification of *Helicobacter pylori*-carcinogenic TNF-alpha-inducing protein inhibitors via daidzein derivatives through computational approaches. *J. Cell. Mol. Med.* **28**, 1-16.
- Lipinski, C. A. 2004. Lead- and drug-like compounds: the rule-of-five revolution. *Drug. Discov. Today Technol.* **1**, 337-341.
- Obot, I. B., Macdonald, D. D. and Gasem, Z. M. 2015. Density functional theory (DFT) as a powerful tool for designing new organic corrosion inhibitors. Part 1: An overview. *Corros. Sci.* **99**, 1-30.
- Vilar, S., Cozza, G. and Moro, S. 2008. Medicinal Chemistry and the Molecular Operating Environment (MOE): Application of QSAR and Molecular Docking to Drug Discovery. *CTMC* **8**, 1555-1572.
- Kim, S. et al. 2016. PubChem Substance and Compound databases. *Nucleic Acids Res.* **44**, D1202-D1213.
- Vargas-Sánchez, R. D., Mendoza-Wilson, A. M., Baladrán-Quintana, R. R., Torrescano-Urrutia, G. R. and Sánchez-Escalante, A. 2015. Study of the molecular structure and chemical reactivity of pinocembrin by DFT calculations. *Comput. Theor. Chem.* **1058**, 21-27.
- Knight, M. L. et al. 2021. Structure of an H3N2 influenza virus nucleoprotein. *Acta Crystallogr. F: Struct. Biol. Commun.* **77**, 208-214.

31. Johansson, M. U., Zoete, V., Michielin, O. and Guex, N. 2012. Defining and searching for structural motifs using DeepView/Swiss-PdbViewer. *BMC Bioinformatics* **13**, 1-11.
32. Dallakyan, S. and Arthur J. Olson. 2015. Small-Molecule Library Screening by Docking with PyRx. in *Chem. Biol. Methods Protoc.* pp.243-250.
33. Schlegel, H. B. 2011. Geometry optimization. *WIREs Comput. Mol. Sci.* **1**, 790-809.
34. Daina, A., Michielin, O. and Zoete, V. 2017. SwissADME: a free web tool to evaluate pharmacokinetics, drug-likeness and medicinal chemistry friendliness of small molecules. *Sci. Rep.* **7**, 1-12.
35. Roux, M. V., Temprado, M., Chickos, J. S. and Nagano, Y. 2008. Critically Evaluated Thermochemical Properties of Polycyclic Aromatic Hydrocarbons. *J. Phys. Chem. Ref. Data.* **37**, 1855-1996.
36. Lien, E. J., Guo, Z.R., Li, R.L. and Su, C.T. 1982. Use of dipole moment as a parameter in drug-receptor interaction and quantitative structure-activity relationship studies. *J. Pharm. Sci.* **71**, 641-655.
37. Ramalingam, S., Karabacak, M., Periandy, S., Puviarasan, N. and Tanuja, D. 2012. Spectroscopic (infrared, Raman, UV and NMR) analysis, Gaussian hybrid computational investigation (MEP maps/HOMO and LUMO) on cyclohexanone oxime. *Spectrochim. Acta Part A: Mol. Biomol. Spectrosc.* **96**, 207-220.
38. Obot, I. B., Macdonald, D. D. and Gasem, Z. M. 2015. Density functional theory (DFT) as a powerful tool for designing new organic corrosion inhibitors. Part 1: An overview. *Corros. Sci.* **99**, 1-30.
39. Zhuo, L., Liao, W. and Yu, Z. 2012. A frontier molecular orbital theory approach to understanding the mayr equation and to quantifying nucleophilicity and electrophilicity by using HOMO and LUMO energies. *Asian J. Org. Chem.* **1**, 336-345.
40. Nile, S. H. et al. 2022. Chemical composition, cytotoxic and pro-inflammatory enzyme inhibitory properties of *Withania somnifera* (L.) Dunal root extracts. *S. Afr. J Bot* **151**, 46-53.
41. Ramalingam, S., Karabacak, M., Periandy, S., Puviarasan, N. and Tanuja, D. 2012. Spectroscopic (infrared, Raman, UV and NMR) analysis, Gaussian hybrid computational investigation (MEP maps/HOMO and LUMO) on cyclohexanone oxime. *Spectrochim. Acta Part A: Mol. Biomol. Spectrosc.* **96**, 207-220.
42. Scrocco, E. and Tomasi, J. 2005. The electrostatic molecular potential as a tool for the interpretation of molecular properties. in *New Concepts II* (Springer, Berlin, Heidelberg, pp.95-170
43. Fischer, A., Smieško, M., Sellner, M. and Lill, M. A. 2021. Decision making in structure-based drug discovery: visual inspection of docking results. *J. Med. Chem.* **64**, 2489-2500.
44. El-Demerdash, A. et al. 2021. Investigating the structure-activity relationship of marine natural polyketides as promising SARS-CoV-2 main protease inhibitors. *RSC Adv.* **11**, 31339-31363.
45. Cichero, E., Calautti, A., Francesconi, V., Tonelli, M., Schenone, S. and Fossa, P. 2021. Probing in silico the benzimidazole privileged scaffold for the development of drug-like anti-rsv agents. *Pharmaceuticals* **14**, 1-29.
46. Lipinski, C. A., Lombardo, F., Dominy, B. W. and Feeney, P. J. 2001. Experimental and computational approaches to estimate solubility and permeability in drug discovery and development settings1. *Adv. Drug Deliv. Rev.* **46**, 3-26.
47. Lipinski, C. A. 2000. Drug-like properties and the causes of poor solubility and poor permeability. *J. Pharmacol. Toxicol. Methods* **44**, 235-249.
48. Chillistone, S. and Hardman, J. G. 2017. Factors affecting drug absorption and distribution. *Anaesth. Intensive Care Med.* **18**, 335-339.
49. Mikov, M. et al. 2017. The role of drug metabolites in the inhibition of cytochrome p450 enzymes. *Eur. J. Drug. Metab. Pharmacokinet.* **42**, 881-890.
50. Yan, Z. and Caldwell, G.W., 2013. *In vitro* identification of cytochrome P450 enzymes responsible for drug metabolism. in *Methods and Protocols*, pp.251-261.
51. Feng, B., LaPerle, J. L., Chang, G. and Varma, M. V. 2010. Renal clearance in drug discovery and development: molecular descriptors, drug transporters and disease state. *Expert. Opin. Drug Metab. Toxicol.* **6**, 939-952.
52. Fuse, E., Kobayashi, T., Inaba, M. and Sugiyama, Y. 1995. Prediction of the maximal tolerated dose (MTD) and therapeutic effect of anticancer drugs in humans: integration of pharmacokinetics with pharmacodynamics and toxicodynamics. *Cancer Treat. Rev.* **21**, 133-157.
53. Hutchinson, T. H., Bögi, C., Winter, M. J. and Owens, J. W. 2009. Benefits of the maximum tolerated dose (MTD) and maximum tolerated concentration (MTC) concept in aquatic toxicology. *Aquat. Toxicol.* **91**, 197-202.